



**UvA-DARE (Digital Academic Repository)**

**Characterisation of polymeric network structures**

Peters, R.

[Link to publication](#)

*Citation for published version (APA):*

Peters, R. (2009). Characterisation of polymeric network structures Maastricht: Universitaire Pers Maastricht

**General rights**

It is not permitted to download or to forward/distribute the text or part of it without the consent of the author(s) and/or copyright holder(s), other than for strictly personal, individual use, unless the work is under an open content license (like Creative Commons).

**Disclaimer/Complaints regulations**

If you believe that digital publication of certain material infringes any of your rights or (privacy) interests, please let the Library know, stating your reasons. In case of a legitimate complaint, the Library will make the material inaccessible and/or remove it from the website. Please Ask the Library: <http://uba.uva.nl/en/contact>, or a letter to: Library of the University of Amsterdam, Secretariat, Singel 425, 1012 WP Amsterdam, The Netherlands. You will be contacted as soon as possible.

## 2

## Characterisation of UV-cured acrylate networks by means of hydrolysis followed by aqueous size-exclusion combined with reversed-phase chromatography

### Abstract

UV-cured networks prepared from mixtures of bi-functional polyethylene glycol di-acrylate and mono-functional 2-ethylhexyl acrylate were analysed after hydrolysis, by aqueous size-exclusion chromatography coupled to on-line reversed-phase liquid-chromatography. The mean network density and the fraction of dangling chain ends of these networks were varied by changing the concentration of mono-functional acrylate. The amount and the molecular weight distribution of the polyethylene glycol chains between cross-links and polyacrylic acid backbone chains (the so-called kinetic chain length, *kcl*) in the different acrylate networks were determined quantitatively. The molecular weight distribution of *kcl* revealed an almost linear dependence on the concentration of mono-functional acrylate. Analysis of the starting materials showed a significant concentration of mono-functional polyethylene glycol acrylate. In combination with the analysis of the extractables of the UV-cured networks, more insight in the total network structure was obtained. It was shown that the UV-cured networks contain only small fractions of residual compounds. With these results, the chemical network structure for the different UV-cured acrylate polymers was expressed in network parameters such as the number of polyacrylic acid units which are cross-linked, the degree of cross-linking, and the network density. The mean molecular weight of chains between chemical network junctions was calculated and compared with results obtained from solid-state nuclear-magnetic resonance and mechanical analysis. The mean molecular weight of chains between network junctions as determined by these methods was similar.

*R. Peters, V.M. Litvinov, P. Steeman, A.A. Dias, Y. Mengerink, R. van Benthem, C.G. de Koster, Sj. van der Wal, P. Schoenmakers, Journal of Chromatography A, 1156 (2007) 111–123.*

## 2.1. Introduction

UV-curing remains one of the most effective processes to produce instantaneously highly cross-linked acrylate materials. The solvent-free and the high-rate of curing reaction and the ease of applicability are the main advantages of photo-curing. In general, the network structure determines the mechanical and elastic properties of cross-linked acrylate polymers. Typical examples of these properties are modulus, strain hardening, tear strength, creep, and glass-rubber transition temperature ( $T_g$ )[1]. UV-cured acrylate polymers have a broad application field, including optical storage, optical display, and increasingly as biomedical materials. The network structure is a consequence of the acrylates used and the kinetics of this cross-linking polymerisation. This determines the mean molecular weight of visco-elastic chains between network junctions, type of network junctions and network imperfections. To be able to improve the performance of cross-linked polymers formed by free-radical polymerisation, the relation between the chemical network structure and the final network properties must be elucidated. An interesting well-studied type of cross-linked acrylate polymer is a photo-cured mixture of bi-functional polyethylene glycol di-acrylate (PEGDA) and mono-functional 2-ethylhexyl acrylate (EHA)(see *Fig. 2.1*). These acrylates react to degradable cross-linked networks, which have many benefits as biomedical materials [2]. The mean network density and the fraction of dangling chain ends of the acrylate network can be changed by varying the concentration of mono-functional acrylate. An increase in the concentration of mono-functional monomer causes an increase in the amount of dangling chain ends and a significant decrease in the volume-average network density. This makes these types of networks an ideal case for a study of the chemical network structure. Since these kinds of polymers may be intended to be used as biomedical materials, the study of the chemical network structure is even more important. In the case of the present UV-cured PEGDA/EHA networks, polyacrylic acid is one of the degradation products, which is not degraded *in vivo*. Depending on its molecular weight, it may accumulate in the human body [1].

Different approaches have been described to determine the chemical network structure formed by free-radical polymerisation. The chemical conversion can be analysed by spectroscopic techniques such as infrared (IR) or nuclear-magnetic resonance (NMR) spectroscopy [3,4]. The conversion is usually closely related to the degree of cross-linking. However, no quantitative information about the network structure can be obtained, since reacted groups can also form different types of ineffective chains, such as dangling chain ends.

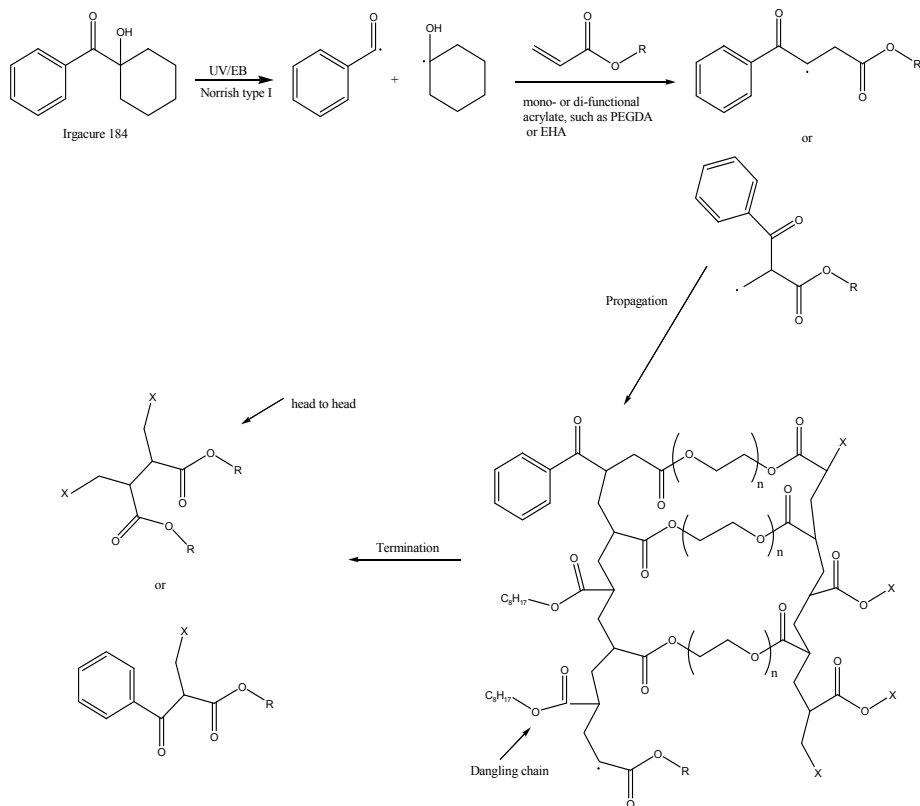


Fig. 2.1. Chemical structures and suggested UV-curing to a highly cross-linked PEGDA/EHA acrylate network.

Time-resolved techniques such as calorimetric or spectrometric methods can be used to monitor the consumption of reactive functionalities during polymerisation as a function of time [5,6]. This gives insight in the chemical conversion during the cross-linking reaction forming the network structure. No distinction can be made between mono- and bi-functional acrylates, although some studies indicate that they have different reactivities [7,8]. The information obtained by these time-resolved techniques can also be used to determine the rates of polymerisation. With this information, the molecular weight distribution of the backbone, which is often denoted as the kinetic chain length ( $kcl$ ) of the network, can be estimated [9–14]. Such an estimate involves several assumptions. As a consequence, the calculated  $kcl$  is only an indicator, which can only be used to interpret general trends [11,15]. A more direct determination of the  $kcl$  can be performed by using “selective” degradation of the network with pyrolysis or hydrolysis, followed by analysis of the volatile or soluble parts by

chromatography. The characterisation of UV-cured acrylic ester polymers by pyrolysis-gas chromatography-mass spectrometry (Pyr-GC-MS) has been described by Matsubara *et al.* [16] and Matsubara and Ohtani [17]. Quantitative cleavage of the ester-linkage and limited pyrolytic cleavage of C-C and C-O bonds was observed. The authors suggested that the chain-length distribution of the repeating acryloyl groups could be determined from their results. However, the low recovery of acrylate polymer in GC due to their low volatility and the possible C-C cleavage make the determination of the *kcl* in the UV-cured resin unreliable. The use of hydrolysis followed by chromatography and mass spectrometry to determine the *kcl* of polymeric networks containing an ester-bond, has been demonstrated several times [11,15,18]. The influence of the acrylate conversion and various reaction conditions on the *kcl* has been investigated.

The network can be characterised by physical properties in relation to volume average network density. The most traditional methods are equilibrium swelling and mechanical measurements. Several models have been developed to relate a measured quantity to practical molecular information [1,19], such as molecular weight between cross-links, entanglements molecular weight, and gel content. Several authors demonstrated the practical use of these models. Klein *et al.* use these models for acrylic emulsion pressure-sensitive adhesives to relate various molecular parameters (*e.g.* molecular weight between cross-links from the Flory–Rehner equation) to adhesive performances [20,21], while Colby and co-workers show an elegant application of the percolation theory to non-perfect networks [22]. Another approach to determine the network structure, which is an important network parameter, is the analysis of the network density. In general, the network density is defined as the molar concentration of effective network chains between cross-links (mmol  $XL_c$ ) per volume of polymer [19]. Thus, the network density for “zip-like” PEGDA/EHA networks can be expressed as the number of mols of polyethylene glycol chains per volume of polymer. In practice, the network density is specified depending on the way in which it has been determined. For example, the network density of super-absorbent polymer observed by X-ray microscopy is specified as the optical density [23]. Often, the network density is expressed as the mean molecular weight of network chains between chemical and physical network junctions ( $M_{C+e}$ ) [24,25]. The  $M_{C+e}$  can be analysed by different spectroscopic techniques. Solid-state-NMR (s-NMR) in particular provides useful information regarding this network parameter [26,27]. Different types of s-NMR relaxation experiments can be used to determine the mobility of polymeric chains, which is strongly related to the length of network chains and thus to the network density [28]. The mobility of network chains can

be measured by the relaxation time at 100–150°C above  $T_g$ , where it is sensitive to the conformational mean position of network chains, which depends on the number of statistical segments between chemical and physical network junctions. The relaxation time at these temperatures ( $T_2$ ) has been quantitatively related to the number of statistical segments in network chains, which can be used to calculate  $M_{C+e}$  [27]. The relation between  $T_2$  and  $M_{C+e}$  is based on models, which are derived for perfect low density networks of Gaussian-distributed chains, cross-linked with tri-functional cross-linkers [27]. Despite this restriction, the  $M_{C+e}$  values of cross-linked PEGDA/EHA networks with “zip-like” network junctions were determined by s-NMR. Although a large uncertainty is present in values used in the models [26,29], a good agreement was obtained with  $M_{C+e}$  values determined by dynamic mechanical analysis (DMA, see below). The characterisation of structural parameters, such as the  $kcl$  has not yet been achieved by s-NMR. Another approach is to use DMA to characterise the network. These measurements yield practical information, such as the storage modulus ( $E'$ ) and  $T_g$ , which can also be used to determine the density of cross-links [30]. The  $M_{C+e}$  value of cross-linked homogeneous networks, with Gaussian-chain statistics, can be calculated from the slope of the linear part of the temperature dependence of the modulus ( $E'/T$ ) at temperatures above the  $T_g$  [31–33]. In the case of heterogeneity, such as highly cross-linked micro-gel particles embedded in a less cross-linked matrix, the relation is not valid, since largely heterogeneous networks cannot be analysed using classical rubber-elasticity theories.

The approaches described above have provided many valuable insights into UV-cured acrylate networks. However, most of the described methods are based on models for perfect networks. Moreover, s-NMR and DMA do not yield any detailed information on the network structure in terms of concentration and molecular weight distribution of network chains, such as the kinetic chain length,  $kcl$  [34]. The relation between  $kcl$  and the network structure determined with s-NMR and DMA is limited [31]. The determination of network parameters with chromatography is not straightforward, since cross-linked polymers have an insoluble three-dimensional network structure. In the case of highly cross-linked PEGDA/EHA acrylates, selective scission of the ester-bonds by hydrolysis releases polyethylene glycol (PEG), which represents the chain between cross-links junctions ( $XL_c$ ), and polyacrylic acid (PAA), which represents the acrylate backbone chain ( $kcl$ ). The concentration and distribution (weight-average molecular weight ( $M_w$ ) and number-average molecular weight ( $M_n$ )) of PEG and PAA after hydrolysis can be determined with aqueous size-exclusion chromatography (SEC) [35–38]. Possible co-elution of the two

polymers with each other and/or with other compounds (*e.g.* salts) makes the simultaneous characterization of PAA and PEG less accurate. To improve the separation between PAA, PEG and salts from the mixture after hydrolysis, a combination of a separation with aqueous-SEC, followed by on-line reversed-phase liquid-chromatography (LC) was developed (SEC–LC). PAA is eluted by size-exclusion chromatography, while PEG is eluted by both size-exclusion and interaction chromatography.

This chapter describes the development of the SEC–LC separation for PAA and PEG. The method is used to determine the network parameters of highly cross-linked PEGDA/EHA networks with different ratios of mono- and bi-functional acrylates, after hydrolysis. Detailed information on the network structure in terms of concentration and molecular weight distribution of PEG ( $\bar{X}L_c$ ) and PAA ( $kcl$ ) is obtained. To ensure unambiguous interpretation of the hydrolysis-SEC–LC results, the concentration of material not attached to the network was analysed using extractions followed by LC-MS, while the purity of the used acrylate monomers was analysed by LC-MS. The results obtained from the SEC–LC analysis, after hydrolysis, combined with the extraction and purity of the initial compounds, were used to calculate the degree of cross-linking ( $I$ ) as mean number of cross-linked monomeric units of the acrylate backbone chains, the average number of (non-)cross-linked PAA units for each backbone chain, the network density as  $\bar{X}L_c$  per volume of polymer, and the network density as the mean molecular weight of networks chains between chemical network junctions ( $M_C$ ). The same PEGDA/EHA networks were also analysed by DMA and by s-NMR previously [26]. A comparison was made between the network densities ( $M_{C+e}$ ) obtained by DMA and s-NMR, with the network density ( $M_C$ ) obtained by SEC–LC, after hydrolysis.

## 2.2. Experimental

The formulations prior to UV-curing were prepared from mixtures of polyethylene glycol di-acrylate (PEGDA,  $M_n = 700$  Da, Aldrich Chemical Company Inc., Milwaukee, USA) and 2-ethylhexyl mono-acrylate (EHA, Aldrich Chemical Company). The UV-cured acrylate polymers were mixtures of PEGDA and 0, 20, 40, 60 and 100% (*w/w*) EHA. The formulations contained 1% (*w/w*) of photo-initiator 1-hydroxycyclohexyl phenyl ketone (Irgacure 184, Ciba Geigy, Basel, Switzerland). Different ratios of mono- and bi-functional acrylates were used to vary the mean network density by changing the concentration of mono-functional acrylates (EHA), while the reaction of mono-

functional acrylate was studied using 100% (w/w) EHA. The mixtures are designated with numbers (*i.e.* PEGDA/EHA(60:40)), which represent the concentration of the monomers in weight percent. The samples were prepared by curing films of about 0.1 mm thickness on glass plates at 27°C, in a nitrogen atmosphere, on a conveyor belt, fitted with a Fusion F600 (6000W, Fusion UV Systems Inc., Gaithersbrug, USA) electrodeless H-bulb. A UV-dose of 1.5 J/cm<sup>2</sup> (>5.0 W/cm<sup>2</sup>) was measured using an UV Power Puck Light meter (EIT Inc., Virginia, USA). The final conversion of the acrylate networks was measured using ATR-FT-IR. All the cross-linked polymers showed no residual C=C IR signals, which suggest a conversion of >98% (limit of detection), taking in to account that the depth of the IR signals is approximately 1.5 μm. The specific density ( $\rho$ , gr/cm<sup>3</sup>) of the cross-linked mixtures was calculated by assuming weight-average densities of PEGDA (1.11 gr/cm<sup>3</sup>) and EHA (0.86 gr/cm<sup>3</sup>). It has been recognised that a decrease in sample volume (“shrink”) and thus increase in density occurs [39], but this was not included in the calculations.

The hydrolysis of the UV-cured polymers (0.2 gr) was performed in 75 gr NaOH solution (1 M, 24 h, reflux). After hydrolysis a solid silicate remained, which originates from the glass flask (confirmed by IR and XRF). The liquid phase contained no ester (<2%, determined by IR after sample clean-up), indicating complete hydrolysis (>98%) at the conditions used. The polyacrylic acid sodium-salt (PAA-Na) used as a reference material for the hydrolysis experiments had an  $M_w$  of 2000 Da (Aldrich Chemical Company).

The extractions were performed with different solvents, *i.e.* tetrahydrofuran (THF, Biosolve, Valkenswaard, The Netherlands) and acetone (Merck, Darmstadt, Germany). The expensive solvent 1,1,1,3,3,3-hexafluoro-isopropanol (HFIP, Biosolve) was also used as extraction solvent, since it has excellent dissolution properties towards high molecular weight polar polymers at room temperature. The UV-cured polymers (0.1 gr) were finely ground using a mortar and pestle and were extracted with 10.0 mL solvent. The extractions were performed by stirring for 48 h at ambient temperature, since the temperature stability of the polymers was not known. The extraction was finalised with ultrasonic agitation (1 h) (Branson 5210, Danbury, CT, USA). After the extraction, the solvent was evaporated at ambient temperature with dry pure nitrogen gas. The extracts were dissolved in 2.0 mL THF and filtered with a syringe with a filter tip (Spectrum Laboratories Inc., Los Angeles, CA, USA. PP, 0.2 μm, surface area 0.8 cm<sup>2</sup>).

All the chromatographic experiments were performed on an Agilent 1100, equipped with a quaternary pump, degasser, autosampler, column oven, diode-array detector (DAD) with 10 mm cell and a single-quadrupole mass



spectrometry (MS) (Agilent, Waldbronn, Germany). All spectra from 190 to 600 nm (2 nm step size) were stored, while UV-signals at 195, 200, 220, 250, and 280 nm were collected. The MS was run in negative or positive mode with the following conditions:  $m/z$  100–1500, 70V fragmentor, 0.1  $m/z$  step size, 350°C drying gas temperature, 10 L  $N_2$ /min drying gas, 45 psig nebuliser pressure and 4 kV capillary voltage. The LC system was controlled using ChemStation software (A09.01, Agilent). RI detection was performed using a RI-71 detector (Showa Denko KK, Tokyo, Japan) with the following settings: fast response, positive polarity and 512 range. The RI signal was collected with Atlas 2002, version 6.18 data-management system (Thermo LabSystems, Manchester, UK). The equal MS sensitivity of PEG was checked by a  $^1H$ -NMR experiment of approx. 30 mg PEGDA/5 mL  $CDCl_3$  on the Bruker DRX500MHz spectrometer (32 scans, relaxation delay 30 s) at room temperature. All data calculations were performed in a spreadsheet program (Microsoft Excel 2000, Seattle, WA, USA). The analysis of the starting materials and the extractables was performed with an  $250 \times 3$  mm ODS-3 column at 40°C (Inertsil, Varian Inc., Palo Alto, CA, USA) and with a gradient of ultra-pure water (mobile phase A) and acetonitrile (mobile phase B). The gradient was started at  $t = 0$  min with 100% (v/v) A, stayed there for 5 min and changed in 40 min to 100% (v/v) B ( $t = 45$  min). The flow rate was 0.5 mL/min and injection volume was 5  $\mu$ L.

The SEC separations were performed with a highly polar hydroxylated methacrylate  $8 \times 300$  mm Suprema 1000 Å column (10  $\mu$ m particle size), with a separation range of 1–1000  $kDa$  (PSS, Mainz, Germany). The mobile phase (0.1 M  $NH_4Ac$ ) was pumped at a flow rate of 1.0 mL/min. The SEC–LC experiments were performed with the described SEC column and an on-line coupled  $250 \times 4.6$  mm ODS-3 column (Inertsil, Varian Inc., USA). All the SEC–LC conditions were the same as those for stand-alone SEC, except a gradient with acetonitrile (mobile phase B) was used;  $t = 0$  min with 100% (v/v) A, stayed there for 10 min and changed then to 50% (v/v) B at  $t = 30$  min for 5 min (stop time = 120 min). PAA sodium-salt standards (Polymer Laboratories, Shropshire, UK) were used to calibrate the SEC–LC system (see Table 2.1). The calibration curve is given by the relation;  $\log(M) = -0.0271(t_R)^3 + 0.8123(t_R)^2 - 8.6793(t_R) + 36.741$ ,  $R^2 = 0.9977$ . The PAA was calibrated by injection of different standards ( $M_w$  17.800, 37.100 and 83.400  $Da$ ) at different concentrations (0 to 10 mg/gr, corrected for Na concentration). The calibration curve is given by the relation:  $Area(RI) = 255.86(\text{conc.}) - 7.6521$ ,  $R^2 = 0.9995$ . PEG and PEG- $C_4$  were calibrated by injection of different concentrations of hydrolysed PEGDA (initial di-acrylate). The calibration curve shows a non-linear relation with concentration;  $Area(MS) = -3697.9(\text{conc.})^2 + 2886051.9(\text{conc.}) + 8839610$ ,  $R^2 = 0.9967$ .

Table 2.1. Peak-molecular weight ( $M_p$ ), weight-average molecular weight ( $M_w$ ), number-average molecular weight ( $M_n$ ) and PDI of the PAA standards (data supplied by the vendor)

$M_p$ (Da)	$M_w$ (Da)	$M_n$ (Da)	PDI
1250	1930	1230	1.57
2925	3800	2280	1.67
7500	8300	6200	1.34
16000	17800	12800	1.39
28000	37100	22850	1.62
62900	83400	47900	1.74
115000	132500	75900	1.74
323000	440000	251000	1.75
782200	965100	624900	1.54

All solvents and reagents used (methanol, MeOH; acetonitrile, ACN; ammonium acetate,  $\text{NH}_4\text{Ac}$ ; sodium hydroxide, NaOH) were of p.a. quality (Merck, Darmstadt, Germany), while ultra-pure water was obtained from a Milli-Q system (Millipore, Billerica, USA). The 1,1,1,3,3,3-hexafluoroisopropanol was highly pure (Biolsove).

The experimental conditions of the DMA and s-NMR experiments and the calculation of  $M_{C+e}$  for the different PEGDA/EHA networks are described by Litvinov *et al.* [26].

## 2. 3. Results and discussion

### 2.3.1. Analytical results

#### 2.3.1.1. Analysis of the purity of the starting materials

The purity of the starting materials, EHA and PEGDA, is determined by LC-DAD-MS. The UV-chromatograms are shown in Fig. 2.2. EHA shows no impurities using the described LC-MS method, which indicates a high purity (>99%, w/w). PEGDA shows different impurities, such as “free” PEG, which is not involved in any cross-link reaction, and polyethylene glycol mono-acrylate (PEGMA), which forms dangling chain ends. Besides PEG and PEGMA, an additional series of bi-functional acrylate was identified as PEGDA- $\text{C}_4$  ( $\text{H}_2\text{C}=\text{CH}-\text{CO}-(\text{O}-\text{CH}_2-\text{CH}_2)_n-(\text{O}-\text{CH}_2-\text{CH}_2-\text{CH}_2-\text{CH}_2)-\text{O}-\text{CO}-\text{CH}=\text{CH}_2$ ). The concentration of impurities is quantified, based on the calibration factor of

PEGDA corrected for the UV-contribution of the acrylate endgroups [40]. The determined purity of the used PEGDA is 78.4% (w/w) (see Table 2.2).

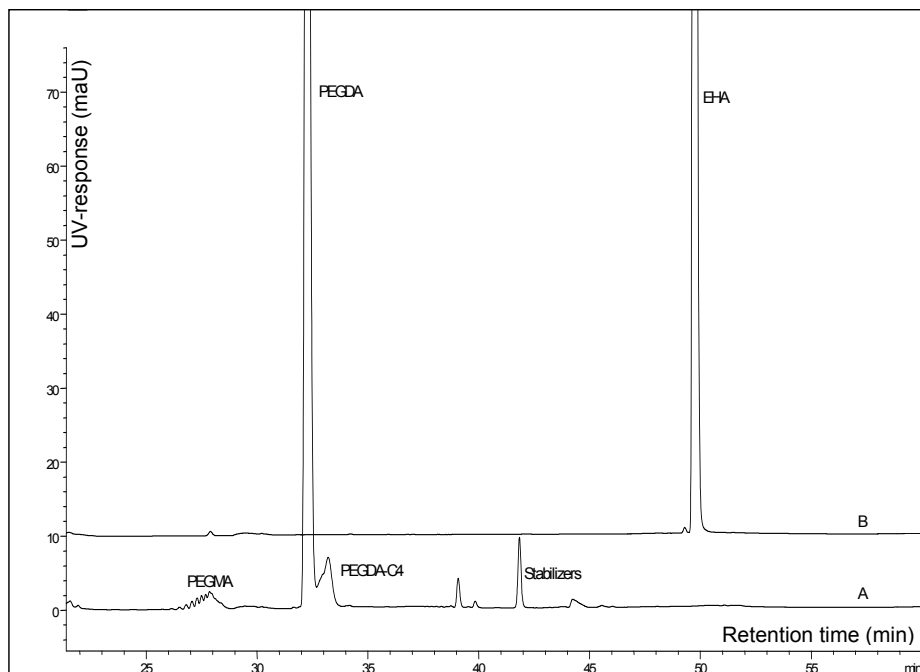


Fig. 2.2. UV-chromatogram ( $\lambda = 210$  nm) of PEGDA (A) and EHA (B). Conditions: 250 $\times$ 3 mm ODS-3, 0.5 mL/min, 40°C, 5  $\mu$ L, gradient; 0–5 min, 100% H<sub>2</sub>O, 5–45 min from 0–100% acetonitrile, where it remains constant for 15 min.

Table 2.2. Impurities of the used PEGDA ( $M_n$  of  $\sim$ 700 Da)

Observed mass (Da)	Compound	Conc. (% w/w)
590 $\pm$ n $\times$ 44	H-(O-CH <sub>2</sub> -CH <sub>2</sub> ) <sub>n</sub> -OH (PEG)	2.2
600 $\pm$ n $\times$ 44	H-(O-CH <sub>2</sub> -CH <sub>2</sub> ) <sub>n</sub> -O-CO-CH=CH <sub>2</sub> (PEGMA)	11.8
698 $\pm$ n $\times$ 44	H <sub>2</sub> C=CH-CO-(O-CH <sub>2</sub> -CH <sub>2</sub> ) <sub>n</sub> -O-CO-CH=CH <sub>2</sub> (PEGDA)	78.4
682 $\pm$ n $\times$ 44	H <sub>2</sub> C=CH-CO-(O-CH <sub>2</sub> -CH <sub>2</sub> ) <sub>n</sub> -(O-CH <sub>2</sub> -CH <sub>2</sub> -CH <sub>2</sub> -CH <sub>2</sub> )-O-CO-CH=CH <sub>2</sub> (PEGDA-C <sub>4</sub> )	7.4
710 $\pm$ n $\times$ 44	H <sub>2</sub> C=CH-CO-(O-CH <sub>2</sub> -CH <sub>2</sub> ) <sub>n</sub> -(O-CH <sub>2</sub> -CH <sub>2</sub> -CH <sub>2</sub> -CH <sub>2</sub> -CH <sub>2</sub> ) <sub>2</sub> -O-CO-CH=CH <sub>2</sub> (PEGDA+2 $\times$ C <sub>4</sub> )	< 0.05
716 $\pm$ n $\times$ 44	H-(O-CH <sub>2</sub> -CH <sub>2</sub> ) <sub>n</sub> -(O-CH <sub>2</sub> -CH <sub>2</sub> -CH <sub>2</sub> -CH <sub>2</sub> )-O-CO-CH=CH <sub>2</sub> (PEGMA-C <sub>4</sub> )	< 0.05
--	BHT, mono-ethyl-hydroquinone and others	$\pm$ 0.05

### 2.3.1.2. Determination of $k_{cl}$ and $XI_c$ by SEC-LC

The PAA and PEG in the hydrolysates of the different cross-linked acrylates was analysed by SEC-RI. The RI-chromatograms of the hydrolysed polymers with different PEGDA/EHA ratios are depicted in Fig. 2.3. The chromatograms show PAA and PEG, where the low-molecular weight PEG elutes just in front of solvent peaks around 10.5 min. Various salts elute from the SEC column between 11 and 17 min.

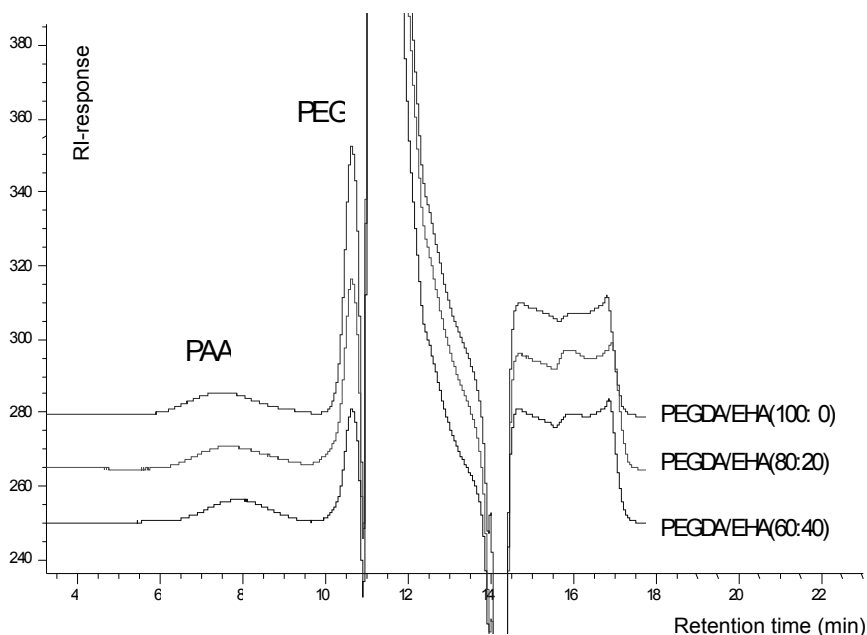


Fig. 2.3. SEC-chromatograms of hydrolysed UV-cured PEGDA/EHA polymers using RI-detection;  $8 \times 300$  mm Suprema column (PSS),  $1000 \text{ \AA}$ ,  $10 \mu\text{m}$ , flow =  $1.0 \text{ mL/min}$   $0.1 \text{ M NH}_4\text{Ac}$ ,  $T = 25^\circ\text{C}$ ,  $V_{inj} = 20 \mu\text{L}$ .

The chromatography of PAA with aqueous SEC can be affected by several parameters such as the ionic strength of the injected sample and the eluent [41]. The influence of the ionic strength of the hydrolysates was investigated by analysing reference PAA ( $M_w = 2 \text{ kDa}$ ) before (dissolved in  $0.1 \text{ M NH}_4\text{Ac}$ ) and after hydrolysis (hydrolysate diluted 1:1 with  $0.1 \text{ M NH}_4\text{Ac}$ ). The RI-chromatograms are given in Fig. 2.4. This experiment demonstrates that the hydrolysis and dilution of the hydrolysis medium with eluent (ratio 1:1) has no effect on the observed PAA peaks in terms of elution time and peak shape. The

influence of the injection volume/mass and the ionic strength of the eluent on the elution time, peak shape and band broadening was investigated by injecting various injection volumes (10–80  $\mu\text{L}$ ) at different ionic strengths (0.1–0.25 M  $\text{NH}_4\text{Ac}$ ), but again no effect was observed.

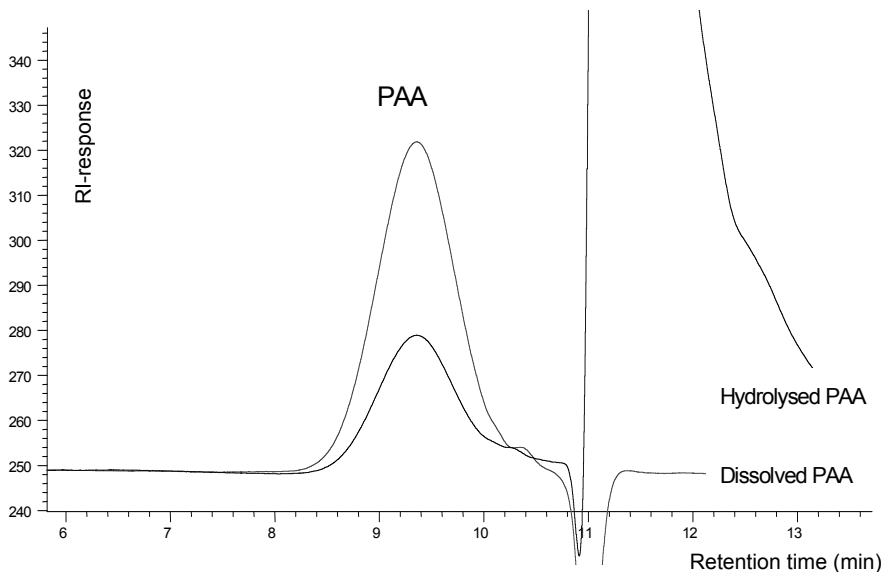


Fig. 2.4. SEC-chromatogram of dissolved and hydrolysed polyacrylic acid ( $M_w$  2 kDa) using RI-detection. Conditions as in Fig. 2.3.

The peaks of PAA and PEG partially overlap with each other, while PEG shows also co-elution with salts. This makes the determination of the molecular weight distributions of PAA and PEG less accurate, especially for the calculation of  $M_n$ , which is strongly affected by the low-molecular-weight side of the peak. In general, the separation of PAA, PEG and salts can be improved by using longer SEC columns with narrower (more dedicated) separation ranges, while the analysis can be improved by selective detection, such as MS-detection. Another way to improve the characterisation of low-molecular weight PEG is the selective removal of salts from the hydrolysates. This was studied by using a dialysis membrane with a molecular weight cut-off of 100 Da. The RI-chromatograms, before and after dialysis of the hydrolysed PEGDA/EHA(80:20), are depicted in Fig. 2.5. The chromatograms demonstrate that, besides the loss of salt, also low-molecular weight PEG is lost from the sample. This rules out dialysis as a sample-preparation method for the characterisation of PEG. However, it also shows that the salts introduced by hydrolysis have no influence on the elution time and peak shape of PAA.

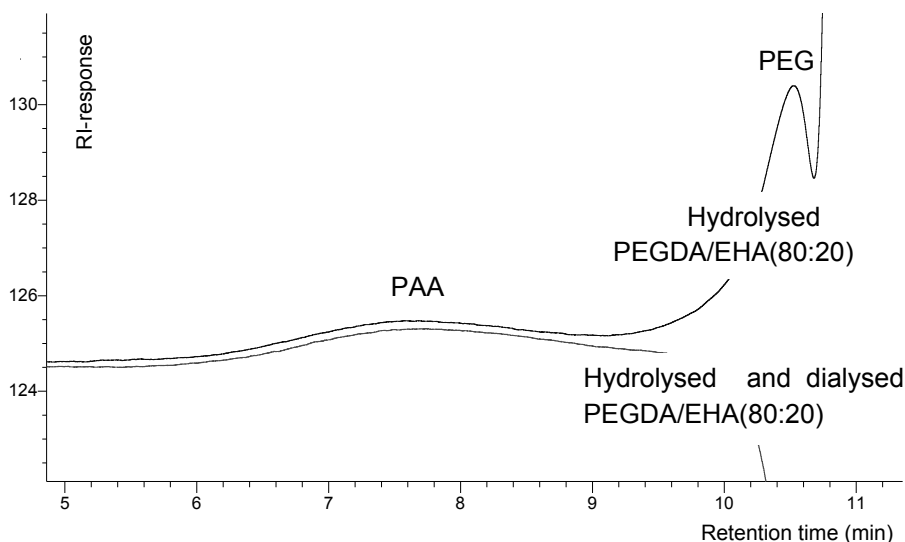


Fig. 2.5. Influence dialysis. SEC-RI chromatogram of hydrolysed PEGDA/EHA (80:20), before and after dialysis. Conditions as in Fig. 2.3.

Instead of using longer SEC columns with a narrower separation range, the separation between PAA and PEG was improved by coupling a SEC column with a reversed-phase LC column (SEC-LC). PAA is separated according to hydrodynamic volume on both columns, while PEG is separated by both size-exclusion and interaction chromatography. Since a gradient was required to elute PEG from the SEC-LC system, RI detection could not be used to detect PEG, while UV-detection is not sensitive due to the low UV-absorbance of PEG. Electrospray ionisation in the positive mode followed by mass spectrometry (ESI(+)-MS) was used to detect PEG. The mass-reconstructed chromatogram of a hydrolysed PEGDA/EHA polymer, analysed with SEC-LC, is shown in Fig. 2.6, while the RI-chromatograms of hydrolysed PEGDA/EHA are given in Fig. 2.7. This shows that PAA elutes under size-exclusion conditions. The SEC-LC separation of PAA and low-molecular weight compounds (such as salts) shows an improvement in resolution, while the different PEG oligomers are totally separated according to their molecular weight and no coelution was observed with salts and PAA. PEG is also separated from an additional PEG series, which is identified as PEG-C<sub>4</sub> (H(-O-CH<sub>2</sub>-CH<sub>2</sub>)<sub>n</sub>-(-O-CH<sub>2</sub>-CH<sub>2</sub>-CH<sub>2</sub>-CH<sub>2</sub>)-OH). This series originates from the PEGDA-C<sub>4</sub> impurity in the PEGDA. The used SEC-LC is not suitable for high-

molecular-weight PEG. To improve the characterisation of PAA, selective on-line MS-detection of PAA was studied. Mass-resolving problems arose for the different molecular weight PAA structures with ESI(-)-MS. The MS-spectra show almost every possible  $m/z$  value, due to the fact that electrospray ionisation of a polydisperse PAA, even after SEC separation, generates multiple negatively charged molecules, with a broad charge distribution. The charge, the molecular weight and the isotope distribution [42], make deconvolution of the molecular weight distribution impossible for broadly distributed PAA. The use of atmospheric pressure chemical ionisation (APCI)-MS, which usually gives single-charge molecular ions, was not investigated, since the mass-range of PAA is much higher than the optimal mass-range of 50–3000  $Da$  for APCI-MS. The low  $S/N$ -ratio, and the generally non-linear response, of PAA make MS-detection less attractive for quantitative PAA detection than RI detection. The molecular weight distributions ( $M_w$ ,  $M_n$ ) of the acrylate backbone chains ( $kcl$ ) and the chains between cross-links ( $XL_c$ ) are characteristic parameters of the UV-cured PEGDA/EHA networks.

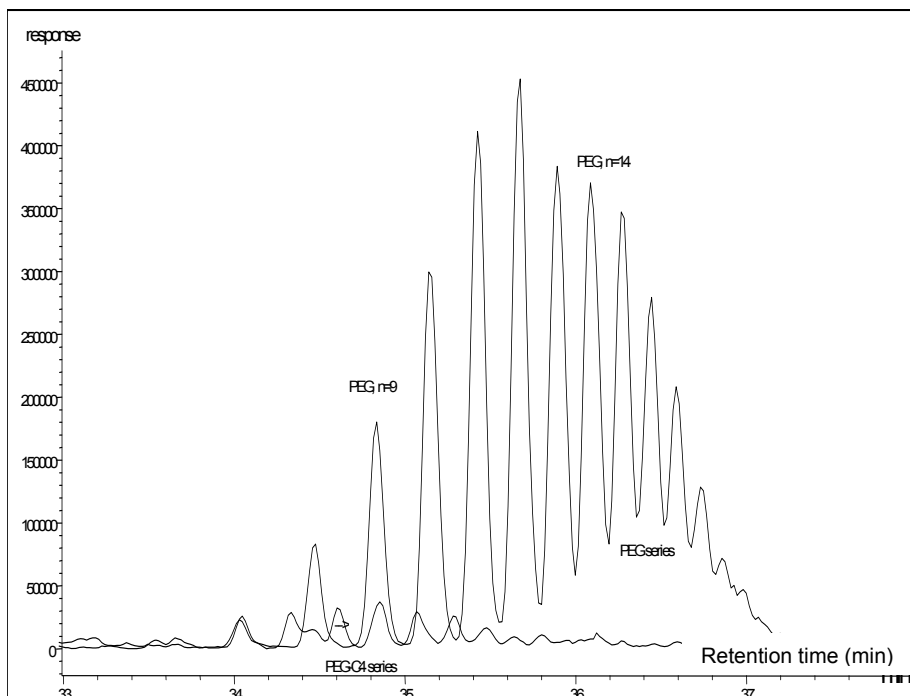


Fig. 2.6. Mass-reconstructed chromatogram of PEG and PEG- $C_4$  of a hydrolysed PEGDA/EHA(60:40) sample analysed by SEC-LC. Conditions;  $8 \times 300$  mm Suprema 1000  $\text{\AA}$  coupled to  $250 \times 4.6$  mm ODS-3 column, 1.0 mL/min, 20  $\mu\text{L}$ , RT, gradient; 0–10 min, 100% 0.1 M  $\text{NH}_4\text{Ac}$ , 10–30 min from 0–50% acetonitrile, where it remains constant for 30 min.

The PAA and PEG in the different hydrolysates were characterised with respect to their molecular weight distribution. The hydrolysates were diluted (1:1) in 0.1 M  $\text{NH}_4\text{Ac}$  and analysed with the described SEC-LC-RI-MS method. The molecular weight distribution characterisation of PAA, using RI-detection, is based on PAA standards. The  $M_w$ ,  $M_n$  and  $PDI$  of PAA in the different samples are given in Table 2.3.

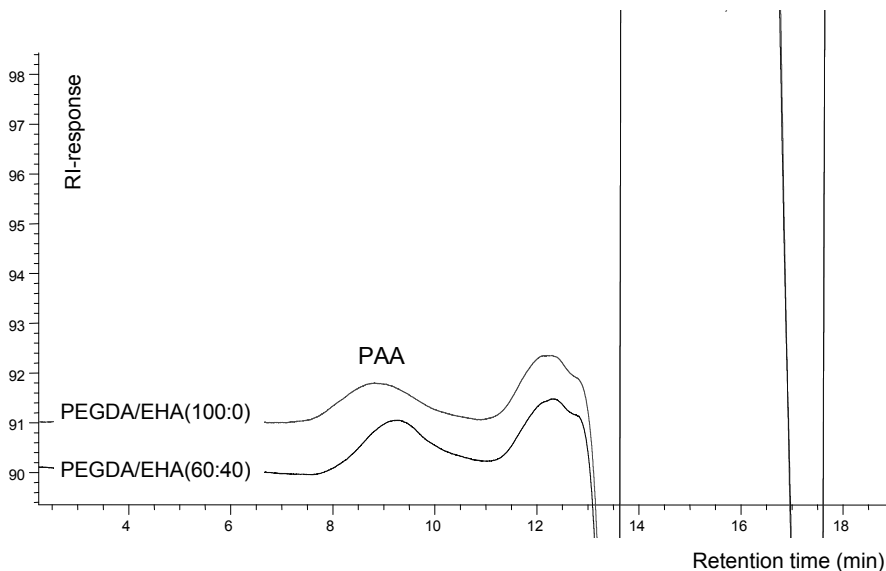


Fig. 2.7. SEC-LC-RI chromatograms of hydrolysed UV-cured acrylates. Conditions as in Fig. 2.6.

Table 2.3. Weight-average molecular weight ( $M_w$ ), number-average molecular weight ( $M_n$ ) and  $PDI$  of PAA, after hydrolysis of the UV-cured acrylate networks

Sample	SEC-LC		
PEGDA/EHA	$M_w$ (Da)	$M_n$ (Da)	$PDI$
100:0	56200	21300	2.6
80:20	46000	18800	2.4
60:40	35700	15500	2.3
40:60	25500	12700	2.0
0:100	7800	4800	1.6

PEG was characterised with MS-detection, assuming equal MS-sensitivity. The PEG has an  $M_w$  of 580 Da and an  $M_n$  of 558 Da. This assumption was checked



by liquid-NMR, where the mol-fraction PEG was determined in the PEGDA starting material, which correspond to an average of 13 PEG units. This makes the assumption of equal MS-sensitivity justified. Since PEG is not the polymerisable group, its  $M_w$  and  $M_n$  are independent of the concentration of PEGDA in the cured polymers. The quantification of PAA, PEG and PEG- $C_4$  was performed using SEC-LC. RI-detection was used to quantify the concentration of PAA, while PEG and PEG- $C_4$  was quantified with ESI(+)-MS detection. The concentrations of PAA, PEG and PEG- $C_4$  are given in *Fig. 2.8*. The concentration of 2-ethyl-1-hexanol is not measured, as it might have been (partially) lost during the sample preparation and, secondly, this value is not required to calculate the network parameters.

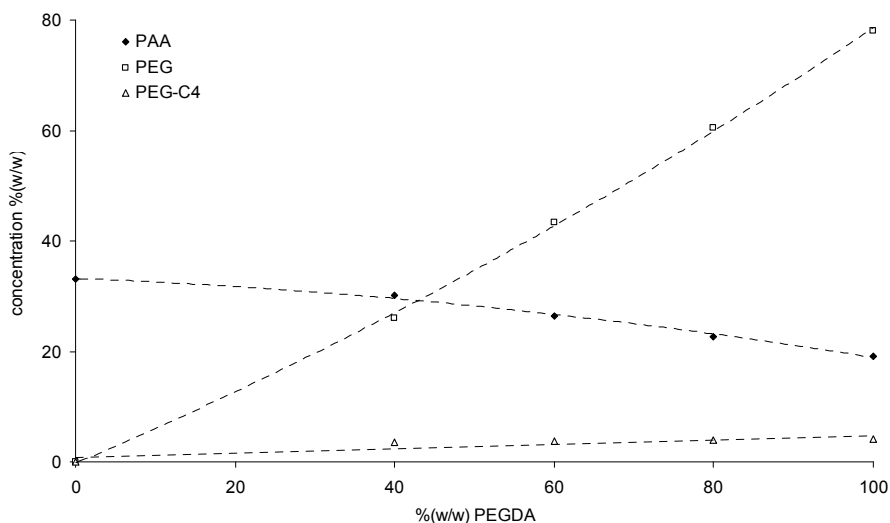


*Fig. 2.8. Total concentration of PEG, PEG- $C_4$  and PAA in UV-cured PEGDA/EHA networks obtained by hydrolysis SEC-LC-RI-ESI(+)-MS, against PEGDA concentration.*

### 2.3.1.3. Analysis of extractables

To complete the picture of the PEGDA/EHA network structure, the concentration of extractables was determined. Since UV-cured PEGDA/EHA(0:100) is not cross-linked, this sample was totally soluble. The soluble fractions from the cured polymers were extracted with THF, acetone or HFIP. The extracted compounds were analysed by LC-DAD-MS. All solvents

show almost the same compounds, but the highest concentration of extracted compounds is observed with HFIP. The extracted compounds are mainly PEG, unreacted EHA, Irgacure 184 and a few unknown compounds at low concentrations (<100 ppm). The UV-spectra of these unknown compounds are almost identical to that of Irgacure 184. These impurities are tentatively identified as Irgacure 184 radicals reacted with EHA. The concentrations of the different extractables versus the concentration of bi-functional acrylates are shown in *Fig. 2.9*.

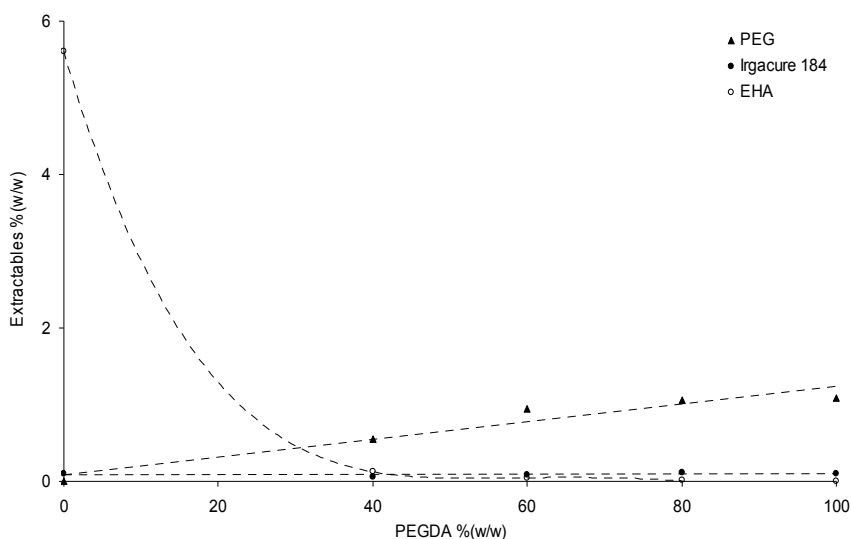


*Fig. 2.9. Concentration of the various compounds extracted from UV-cured PEGDA/EHA networks vs. the concentration of bi-functional acrylate.*

### 2.3.2. Chemical network structure

Analysis of the starting materials shows a significant concentration of impurities in PEGDA, such as “free” PEG, PEGMA and PEGDA-C<sub>4</sub>. UV-cured acrylate networks prepared from EHA and PEGDA, including the determined impurities, show various compounds, which are not attached to the network; such as PEG, EHA, Irgacure 184, and Irgacure reacted with EHA. The concentration of the Irgacure radicals reacted with EHA correlates with the concentration of mono-functional acrylate. The concentration indicates that undesirable reactions occur at low extent during curing. Remarkably, no PEGDA that had reacted with

Irgacure 184 was found, which can be the result of the enhanced reaction rate of PEGDA to higher molecular weight PAA backbone chains. The average concentration of extracted unreacted Irgacure 184 is 0.1% (*w/w*) for all samples, while 1.0% (*w/w*) was added to the formulations before curing. A residual concentration of initiator after the polymerisation is in line with the study of Burdick *et al.* [11], who found high fractions of unused initiator in cured polymers (up to 46%), depending of the light intensity and the concentration of the initiator. Based on the identified compounds, it can be concluded that a significant amount of “free” PEG, introduced in the network as an impurity of PEGDA, is extracted. As one would expect, the concentration of PEG decreases with a decrease in the concentration of PEGDA. The concentration of unreacted EHA is rather low (<0.1%, *w/w*), but it increases rapidly for UV-cured acrylates with a high concentration of EHA (up to 5.6%, *w/w* for PEGDA/EHA(0:100)). The observations are totally in line with the s-NMR results obtained with PEGDA/EHA networks [26], which show similar amounts of a highly mobile fraction. Remarkable is the fact that IR found no residual EHA (<2%, *w/w*) in PEGDA/EHA(0:100), which can be the result of evaporation of the residual EHA on the surface before or during the IR measurement. In general only small concentrations of non-cross-linked compounds were extracted. No extraction recovery was determined for these highly cross-linked polymers, which is difficult to perform. This makes it difficult to draw definitive quantitative conclusions. Quantitative extractions are part of ongoing research. However, the results indicate that the concentration of network defects defined as unreacted material; photo-initiator and side-reactions of photo-initiator are low in these UV-cured PEGDA/EHA networks.

Hydrolysis of the UV-cured acrylate networks, followed by on-line SEC-LC, shows that the concentration of PAA backbone chains increases with a decrease in the concentration of bi-functional acrylate. This is directly related to the number of polymerisable mono- and di-acrylate groups. The  $M_w$  and  $M_n$  of the PAA backbone chains reveal an almost linear dependence on the concentration of bi-functional monomer (see *Fig. 2.10*). The same seems true for the *PDI* of PAA, which is much larger when high concentrations of bi-functional acrylate are used. In general, the *k<sub>cl</sub>* depends on the polymerisation rate and on the bimolecular termination rate [11]. As the initiation of the cross-link reaction is equal for all the different samples (same photo-initiator at same concentration and same light intensity), the concentration of radicals should be equal. This suggests that the initiation rate is similar for all the different PEGDA/EHA polymers. The propagation of the cross-link reaction depends on the polymerisation rate and on the concentration of double bonds, which slightly

increases with increasing concentration of mono-acrylate. As described by Jansen *et al.* [8] the polymerisation rate of PEGDA is higher due to reorganisation by hydrogen bonding and the dipole moment of PEGDA versus EHA. The bimolecular termination rate is higher for EHA, since the polymeric chain has a higher mobility than (partly) cross-linked PEGDA. As one could expect, the differences in propagation and termination of EHA and PEGDA during the cross-link reaction cause a strong decrease in  $kcl$  with increasing concentration of mono-functional acrylate. The relation seems to be non-linear. The  $kcl$  of 100% (w/w) EHA is higher than expected based on the  $kcl$  of UV-cured acrylates with high concentration of bi-functional acrylate. However, the non-linearity may not be significant, given the uncertainty in the determined  $M_w$  and  $M_n$  ( $RSD \sim 5\%$ ).

Based on this data, the chemical structure of UV-cured PEGDA/EHA networks is reconstructed (see Fig. 2.11). The characterisation and quantification of  $kcl$ ,  $XL_c$ , extractables, and impurities indicates that network formation occurs as expected, with the exception that PEGDA- $C_4$  acts also as a cross-linker and that PEGMA forms dangling chain ends. No indications of other network defects were found.

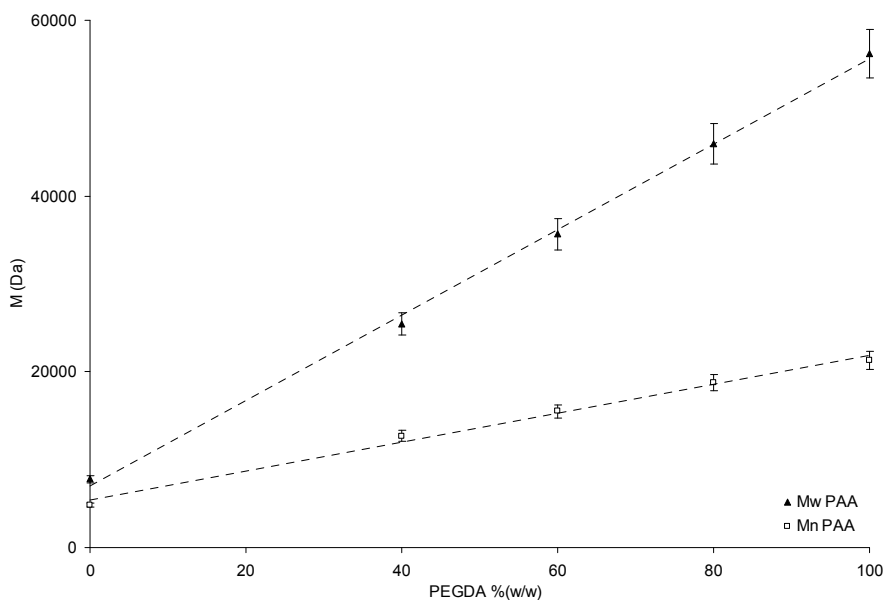


Fig. 2.10. The weight-average and number-average molecular weight of PAA backbone chains in UV-cured PEGDA/EHA networks, obtained by hydrolysis SEC-LC ( $n = 3$ ), against PEGDA concentration.

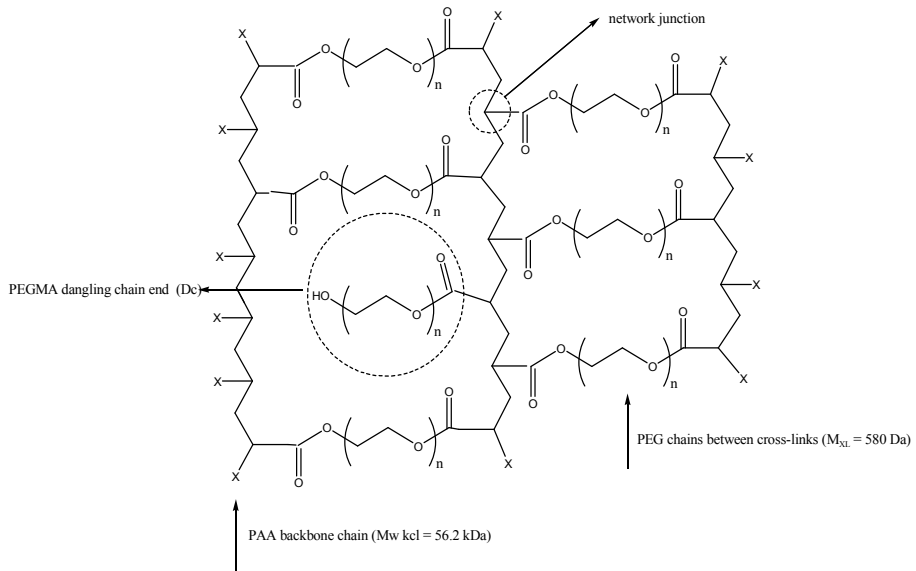


Fig. 2.11a. Chemical network structures of PEGDA/EHA(100:0).

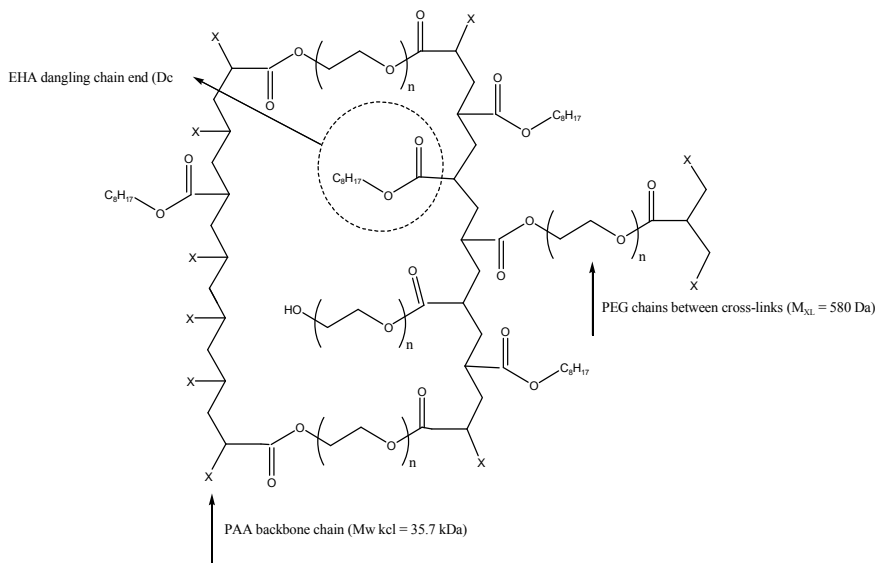


Fig. 2.11b. Chemical network structures of PEGDA/EHA (60:40).

### 2.3.3. Network parameters

Based on the network structure, the degree of cross-linking ( $\Gamma$ ), viz. mean number of cross-linked monomeric units of the primary PAA backbone chains, was calculated using the quantitative and qualitative information on  $kcl$  and  $XL_c$ , as determined by hydrolysis-SEC-LC:

$$\Gamma = \left( \frac{2(c_{PEG} + c_{PEG-C4})I_{PEGDA}}{c_{PAA} \times n_{PAA}} \right) \times 100\% \quad (1)$$

where,  $c_{PAA}$ ,  $c_{PEG}$  and  $c_{PEG-C4}$  are the concentrations (mmol/kg) of PAA backbone chains, PEG, and PEG-C<sub>4</sub> respectively,  $I_{PEGDA}$  is the correction for impurities that do not contribute to the network (weight fraction) in the used PEGDA (0.858) and  $n_{PAA}$  is the average number of PAA units for each network backbone chain, which can be calculated from;

$$n_{PAA} = \left( \frac{M_{n(PAA)} - M_{endgroups}}{M_{PAA}} \right) \quad (2)$$

where  $M_{n(PAA)}$  is the number-average molecular weight of PAA,  $M_{endgroups}$  is the molecular weight of the PAA endgroups ( $2 \times 105 Da$ ), and  $M_{PAA}$  is the molecular weight of the monomeric unit ( $72 Da$ ). The degree of cross-linking is shown in Fig. 2.12. If only PEGDA is used as starting material, the degree of cross-linking is 93%. This results from the impurities in the used PEGDA, such as PEGMA, which form dangling chain ends and do not form cross-links.

To gain more insight in the degree of cross-linking, the number-average of cross-linked and non-cross-linked PAA units of each network backbone chain was calculated. The values are shown in Fig. 2.13. The number of cross-linked PAA units on the backbone chains shows a non-linear decrease with increasing concentration of mono-functional acrylate. The number of non-cross-linked PAA units on the backbone chain, and the increasing concentration of the PAA backbone unit together cause the non-linear degree of cross-linking.

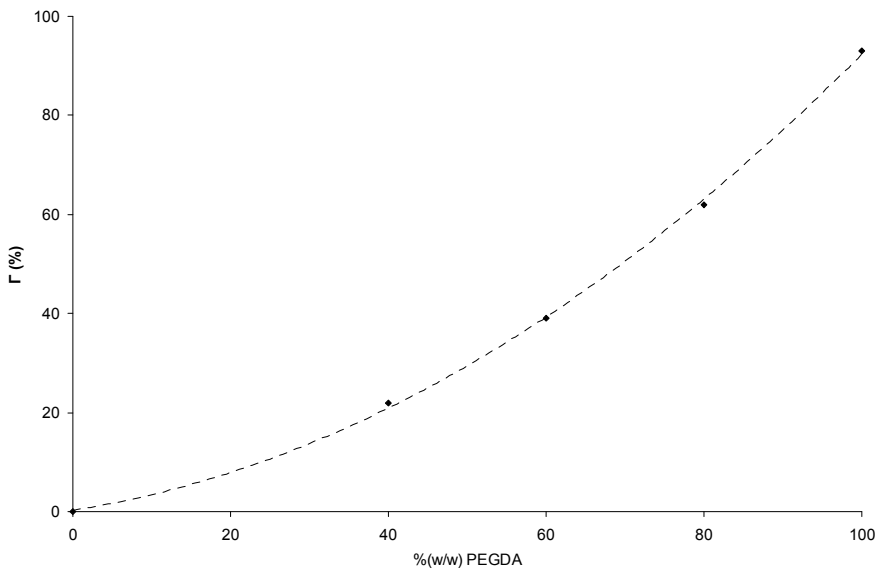


Fig. 2.12. Average degree of cross-linking of the PAA units as calculated by formula 2.1 and 2.2.

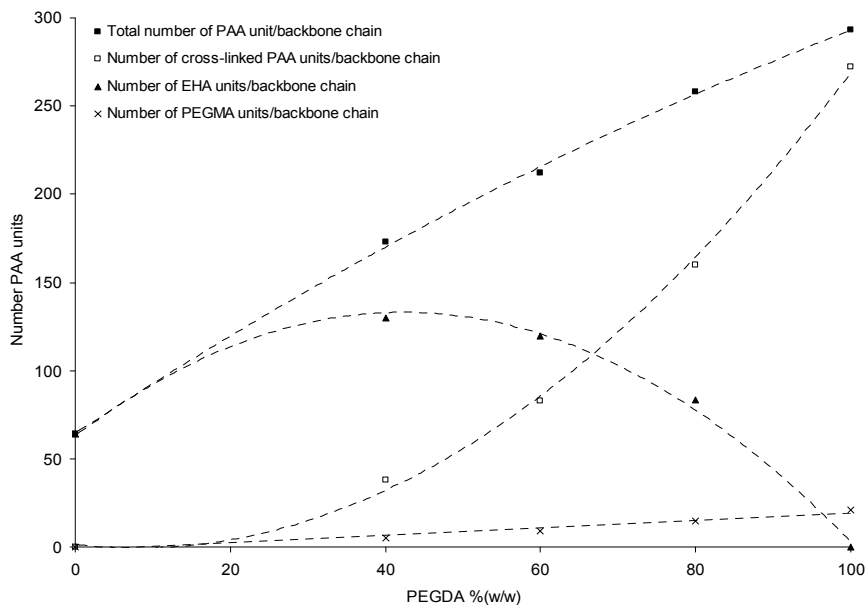


Fig. 2.13. The number of PAA units, cross-linked PAA units and the number of PAA units, which contain a dangling chain end for the different UV-cured PEGDA/EHA networks.

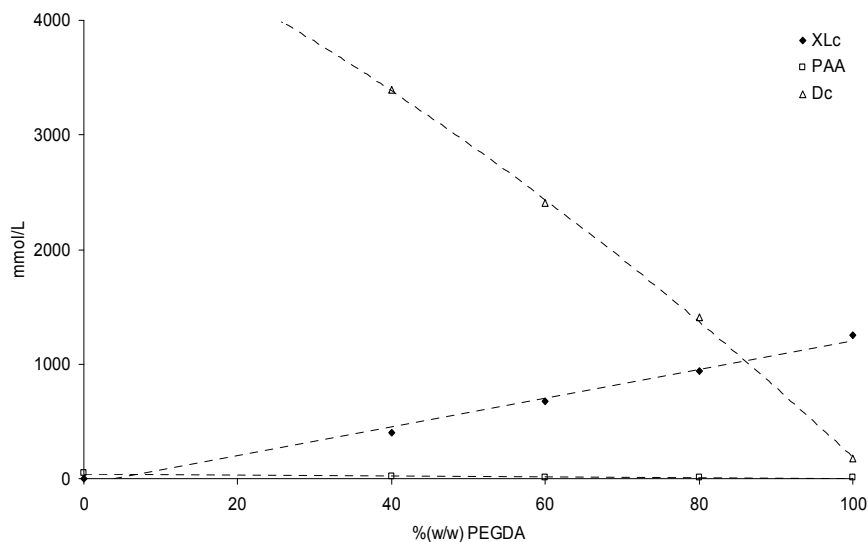


Fig. 2.14. Various parameters of the network for the different UV-cured PEGDA/EHA networks.

### 2.3.4. Comparison of cross-link densities with s-NMR and DMA data

The network densities of the different samples are expressed as mmol PEG and PEG- $C_4$  per volume of polymer, using the determined concentrations and the number-average molecular weight distribution of the visco-elastic PEG chains between network junctions as obtained by hydrolysis SEC-LC. The network density (mmol  $XL_c/L$ ), the number of dangling chain ends (mmol  $D_c/L$ ) and the PAA chains per volume resin (mmol PAA/L), are calculated for the different cured networks. The results are presented in Fig. 2.14. The network density (mmol  $XL_c/L$ ) reveals an almost linear dependence on the concentration of bi-functional acrylate in the mixtures. This shows that “zip-like” network junctions, which are introduced into the networks upon increasing the concentration of bi-functional acrylate cross-linker, influence the network density. The PEGMA impurity in PEGDA causes dangling chain ends. This is the reason why a small fraction of dangling chain ends (mmol  $D_c/L$ ) is still present in PEGDA/EHA(100:0). Due to the high molecular weight of PAA, the PAA concentration (mmol/L) is very low, compared to the value for  $XL_c$ .

The network density is often expressed as  $M_{C+e}$ , which is defined as mean



molecular weight of network chains between physical (temporary entanglements) and chemical network junctions. As shown by Litvinov and Dias [26], these highly cross-linked acrylate networks contain hardly any chain entanglements, which makes  $M_{C+e}$  equal to  $M_C$ . This parameter, as the mean molecular weight of networks chains between chemical network junctions ( $M_C$ ), was calculated from the qualitative and quantitative data on the backbone chains and chains between network junctions obtained by hydrolysis SEC–LC. The determined values were compared with values obtained from s-NMR and DMA. In the present case of “zip-like” network junctions, the  $M_C$  was defined as the mean molecular weight of all the chains between chemical network junctions, including the PAA units with dangling chain ends from EHA or PEGMA. Since we have calculated the degree of cross-linking, molecular weight distribution, and concentration of the different chains, the calculation of the mean molecular weight of network chains between chemical cross-links,  $M_C$ , is possible with;

$$M_C = \left( \frac{2\Gamma M_{PAA} + \Gamma M_{PEG} + 2(100 - \Gamma)M_{non}}{3\Gamma} \right) \quad (3)$$

where  $\Gamma$  is the degree of cross-linking,  $M_{PAA}$  is the molecular weight of the PAA chain between two network junctions (14 Da),  $M_{PEG}$  is the average molecular weight of the PEG chains between network junctions ( $580 - 2 + 2 \times 28 = 634$  Da) and  $M_{non}$  is the molecular weight of the PAA chain between two network junctions, which includes dangling chain ends;

$$M_{non} = \left( \frac{n_{(PEGMA)}(M_{PEGMA} + M_{PAA}) + n_{(EHA)}(M_{EHA} + M_{PAA})}{n_{(PEGMA)} + n_{(EHA)}} \right) \quad (4)$$

where  $n_{(PEGMA)}$  is the mol fraction of PEGMA in PEGDA,  $M_{PEGMA}$  is the molecular weight of the dangling chain ends ( $M = 597$  Da) from PEGMA,  $n_{(EHA)}$  is the mol fraction of EHA calculated from the number of PAA units with EHA dangling chain ends (see also Fig. 2.13) and  $M_{EHA}$  is the molecular weight of the dangling chain ends of EHA ( $M = 157$  Da).

The results of the network density of the different UV-cured PEGDA/EHA acrylates, determined from s-NMR, DMA and hydrolysis-SEC–LC data, are

depicted in *Fig. 2.15*. Since PEGDA/EHA(0:100) is not cross-linked, the network density could not be calculated and is not included in the results. The network density, as  $M_C$ , shows a non-linear dependence on the concentration of bi-functional acrylate, opposite to the trend in the network density as  $\text{mmol } XL_c/L$ , which shows an almost linear dependence on the concentration of bi-functional acrylate. The results of these three different methods are in rather good agreement, especially considering the assumptions [26] made in calculating the network densities from the different techniques. This suggests that classical theories can be used for the calculation of the mean molecular weight of network chains between network junction from the modulus obtained by DMA, for these highly cross-linked acrylate networks which are probably homogenous due to the low-molecular weight of the PEG chain between cross-links [26]. The model used for interpreting the s-NMR also appears to be valid for “zip-like” network junctions, within the large measure of uncertainty [26].

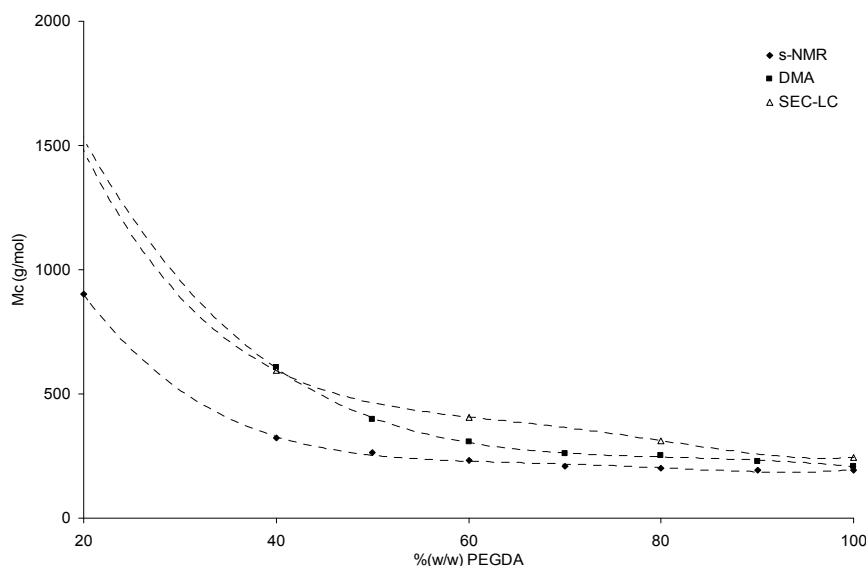


*Fig. 2.15.* The mean molecular weight between chemical cross-links in cured PEGDA/EHA networks against the concentration of mono-functional acrylate.

In general, the network density, expressed as  $M_C$ , decreases with an increase in the concentration of bi-functional acrylate and the correspondingly decreasing numbers of false structures, such as dangling chain ends. Moreover, the  $M_C$  is lower than the mean molecular weight of the PEG chains, which indicates that both s-NMR and DMA account for the different chain structures, such as PAA from EHA.

## 2.4. Conclusion

The UV-cured acrylate networks prepared with different ratios of mono- and bi-functional acrylates were characterised using hydrolysis followed by on-line SEC–LC. The backbone (PAA) chains and the (PEG) chains between network junctions are separated from each other and interfering compounds using SEC–LC, which makes the characterisation in terms of the amounts and molecular weight distributions of PAA and PEG straightforward. Even an additional polymeric series, which were introduced as impurities in the PEGDA, could be analysed. The proposed method provides insight in the kinetic chain length ( $kcl$ ) and chains between cross-linked junctions ( $XL_c$ ) for the different acrylate networks. The  $kcl$  shows an almost linear decrease with increasing amount of mono-functional acrylate. The mono-functional acrylate is part of the  $kcl$  and introduces dangling chain ends. By adding information from extractions, more insight was obtained in the total network structure, including reaction products with the photo-initiator, unreacted monomers, and impurities originating from the starting monomers. The UV-cured networks were found to contain small fractions of residual compounds. From the results of the hydrolysis-SEC–LC analysis, the network structure could be described in terms of different network parameters, such as the number of PAA units which are cross-linked, the number of PAA units which contain dangling chain ends, the degree of cross-linking, and network density (molar concentration of effective network chains between cross-links,  $XL_c$ ) per volume UV-cured polymer. The mean molecular weight of chains between chemical network junctions ( $M_C$ ) was calculated and a good correlation was observed with data from s-NMR and DMA, which suggests that the determination of  $M_C$  with all three methods is correct. Moreover, the  $M_C$  is lower than the mean molecular weight of the PEG chains, which indicates that both s-NMR and DMA account for the different network chain structures, such as PAA from EHA. In general, increasing the fraction of bi-functional acrylate causes a decrease in  $M_C$  and a increase in the molecular weight of the PAA-backbone chains.

## References

- [1] J.F. Rabek, Radiation Curing in Polymer Science and Technology, vol. 1, Elsevier Applied Science, London, 1993.
- [2] A.S. Sawhney, C.P. Pathak, J.A. Hubbell, *Macromolecules* 26 (1993)

- 581.
- [3] A.A. Dias, H. Hartwig, J.F.G.A. Jansen, *Surf. Coat. Int.* 83 (2000) 382.
  - [4] J.L. Koenig, *J. Appl. Polym. Sci.* 70 (1998) 1359.
  - [5] C. Decker, K. Moussa, *Makromol. Chem.* 189 (1988) 2391.
  - [6] P.A.M. Steeman, A.A. Dias, D. Wienke, T. Zwartkruis, *Macromolecules* 37 (2004) 7001.
  - [7] J.E. Elliot, C.N. Bowman, *Macromolecules* 34 (2001) 4642.
  - [8] J.F.G.A. Jansen, A.A. Dias, M. Dorschu, B. Coussens, *Macromolecules* 36 (2003) 3861.
  - [9] C. Decker, K. Moussa, *Eur. Polym. J.* 27 (1991) 881.
  - [10] C. Decker, K. Moussa, *Eur. Polym. J.* 27 (1991) 403.
  - [11] J.A. Burdick, T.M. Lovestead, K.S. Anseth, *Biomacromolecules* 4 (2003) 149.
  - [12] K.S. Anseth, C.N. Bowman, *Polym. React. Eng.* 4 (1992–1993) 499.
  - [13] M.D. Goodner, H.R. Lee, C.N. Bowman, *Ind. Eng. Chem. Res.* 36 (1997) 1247.
  - [14] K.A. Berchtold, T.M. Lovestead, C.N. Bowman, *Macromolecules* 35 (2002) 7968.
  - [15] A.K. Burkoth, K.S. Anseth, *Macromolecules* 32 (1999) 1438.
  - [16] H. Matsubara, A. Yoshida, Y. Kondo, S. Tsuge, H. Ohtani, *Macromolecules* 36 (2003) 4750.
  - [17] H. Matsubara, H. Ohtani, *J. Anal. Appl. Pyrolysis* 75 (2006) 226.
  - [18] J.B. Hutchison, A.S. Lindquist, K.S. Anseth, *Macromolecules* 37 (2004) 3823.
  - [19] P. Flory, J. Rehner, *J. Phys. Chem.* 11 (1943) 512.
  - [20] S.D. Tobing, A. Klein, *J. Appl. Polym. Sci.* 79 (2001) 2230.
  - [21] S.D. Tobing, A. Klein, *J. Appl. Polym. Sci.* 79 (2001) 2558.
  - [22] S.K. Patel, S. Malone, C. Cohen, J.R. Gillmor, R.H. Colby, *Macromolecules* 25 (1992) 5241.
  - [23] G.E. Mitchell, L.R. Wilson, M.T. Dineen, S.G. Urquhart, F. Hayes, E.G. Righthor, A.P. Hitchcock, H. Ade, *Macromolecules* 35 (2002) 1336.
  - [24] R. Schwalm, L. Haussling, W. Reich, E. Beck, P. Enenkel, K. Menzel, *Prog. Org. Chem.* 32 (1997) 191.
  - [25] H. Stutz, K.H. Illers, J. Mertens, *J. Polym. Sci., Part B: Polym. Phys.* 28 (1990) 1483.
  - [26] V.M. Litvinov, A.A. Dias, *Macromolecules* 34 (2001) 4051.
  - [27] C.G. Fry, A.C. Lind, *Macromolecules* 21 (1988) 1292.
  - [28] V.J. McBirtly, K.J. Packer, *Nuclear Magnetic Resonance in Solid Polymers*, Cambridge University Press, 1993.
  - [29] K. Saalwachter, *Macromolecules* 38 (2005) 1508.
  - [30] J.T. Seitz, *J. Adv. Polym. Sci.* 49 (1993) 1331.
  - [31] L.R.G. Treloar, *The Physics of Rubber Elasticity*, third ed., Clarendon Press, Oxford, 1975.
  - [32] G. Heinrich, E. Straube, G. Helmig, *J. Adv. Polym. Sci.* 85 (1988) 33.
  - [33] P.J. Flory, *Principles of Polymer Chemistry*, Cornell University Press,

- Ithaca, N Y, 1953.
- [34] S.M. Gasper, D.N. Schissel, L.S. Baker, D.L. Smith, R.E. Younman, L.-M. Wu, S.M. Sonner, R.R. Hancock, C.L. Hogue, S.R. Givens, *Macromolecules* 39 (2006) 2126.
  - [35] W.W. Yau, J.J. Kirkland, D.D. Bly, *Modern Size-exclusion Liquid Chromatography*, Wiley, New-York, 1979.
  - [36] P.L. Dublin, *Aqueous Size-Exclusion Chromatography*, Elsevier, *J. Chromatogr. Libr.*, 40, 1988.
  - [37] S.S. Cutie, S.J. Martin, *J. Appl. Polym. Sci.* 55 (1995) 605.
  - [38] W.S. Bahary, M. Jilani, *J. Appl. Polym. Sci.* 48 (1993) 1531.
  - [39] K.S. Anseth, C.N. Bowman, N.A. Peppas, *J. Appl. Polym. Sci.* 32 part A (1994) 139.
  - [40] Y. Mengerink, R. Peters, M. Kerkhoff, J. Hellenbrand, H. Omloo, J. Andrien, M. Vestjens, S.J. van der Wal, *J. Chromatogr. A* 878 (2000) 45.
  - [41] D.J. Nagy, *J. Appl. Polym. Sci.* 59 (1996) 1479.
  - [42] Y. Mengerink, R. Peters, C.G. de Koster, S.J. van der Wal, C.A. Cramers, *J. Chromatogr. A* 914 (2000) 131.